UNIVERSIDAD DE LAS AMÉRICAS PUEBLA

Engineering School

Chemical and Food Engineering Department

Mathematical model of methane jet diffusion flames in sub-atmospheric and atmospheric pressures

Scientific Article that to complete the requirements of the Honors Program presents the student

Jonathan García Hilarios

149778

***Licenciatura* in Chemical Engineering & Environmental Engineering**

Advisor: Adriana Palacios Rosas, Ph.D.

San Andrés Cholula, Puebla. **Spring 2019**

Signature sheet

Scientific Article that to complete the requirements of the Honors Program presents the student **Jonathan Garcia Hilarios, ID: 149778**

Advisor

_____

Adriana Palacios Rosas, Ph.D.

President

_____

Deborah Xanat Flores Cervantes, Ph.D.

Secretary

_____

Ernestina Moreno Rodriguez, Ph.D.

MATHEMATICAL MODEL OF METHANE JET DIFFUSION FLAMES IN SUB-ATMOSPHERIC AND ATMOSPHERIC PRESSURES

Jonathan Garcia Hilarios
Departamento de Ingeniería Química y Alimentos
Universidad de las Américas Puebla
San Andrés Cholula, Puebla 72810, México.
Mayo 2019

Abstract:

Flame jets are fire characterized by a turbulent diffusion flame resulting from the combustion of fuel being continuously released with a significant impulse in a particular direction. In this study, geometric parameters of the flame are determined by experiments in a sub-atmospheric chamber at pressures of 0.7 atm, 0.8 atm, 0.9 atm and 1 atm at a flow of 10.24 liters per minute in transitory regime. The geometric parameters of interest are flame diameter, visible flame height, total height, lift off distnce and flame volume. Also, these geometric parameters are related to dimensionless numbers and mathematical models are suggested. Finally, it is concluded that the effect of the pressure is significant on the geometric parameters of the flame and further investigations should be carried out to compliment this case study.

Keywords: *Jet Flames, Lift off Distance, Visible Flame Height, Flame Volume, Subatmospheric.*

Resumen:

Los dardos de fuego o *jets flames* son un tipo de fuego que se caracteriza por una llama de difusión turbulenta resultante de la combustión de un combustible continuamente liberado con un impulso significativo en una dirección particular. En este estudio, se determinan parámetros geométricos de la llama mediante experimentos en una cámara a condiciones subatmosféricas a las presiones de 0.7 atm, 0.8 atm, 0.9 atm y 1 atm a un flujo de 10.24 litros por minuto en régimen transitorio. Los parámetros geométricos de interés son el diámetro, altura radiante, altura total, altura de despegue y el volumen la llama. Asimismo, estos parámetros geométricos se relacionan con números adimensionales y se determina el efecto de la presión sobre los resultados. Finalmente, se presenta modelos empíricos de los datos experimentales que modelan los parámetros geométricos y se concluye que el efecto de la presión es significativo sobre los parámetros geométricos de las llamas.

Palabras Clave: *Dardos de Fuego, Distancia de Despegue, Altura Radiante de Llama, Volumen de Llama, Subatmosférico.*

1. Introduction

1.1. Jet Flames: Domino effect in accidents sequences

A seemingly controlled accident at a process plant or transportation site, such as a minor fire; can wreak havoc to other surrounding equipment. For instance, flames surrounding a vessel may lead to an explosion that could result in the ejected fragments breaking another pipe, damaging equipment or even resulting in injured people. Overall, a minor accident that can be easily prevented or controlled, may lead to an accident sequence with serious consequences for both; equipment and people. This phenomenon is known as the domino effect.

Casal (2018) defines the domino effect as the propagation of an accident to one or more units or plants, in which secondary accidents are triggered in sequence as a result of the primary event; with secondary accidents being more severe than the primary one. Moreover, domino effect is important in process industry as safety measures can be identified by correctly categorizing this phenomenon.

Furthermore, various versions of the European Union Seveso Directive, particularly in Seveso-III, has specifically addressed domino effect in risks analysis, in order to establish safety standards for the prevention of serious industrial accidents involving hazardous substances. Among the most common accidents leading to severe equipment failure are jet flame impingement, pool fires, boiling liquid expanding vapor explosions (BLEVEs), and the impact of explosion missiles (Casal, 2018).

Although these phenomena can occur in any industrial installation, facilities whereas processing equipment and control systems are near to each other, are especially prone to these types of primary event. Moreover, Darbra et al. (2010) analysis suggest that most (35%) domino accidents occur at storage areas, followed by process plants (28%), and transportation (19%).

Pool fires and jet fires only transfer heat by thermal radiation reaching the target, or direct contact between the flames and the target; nevertheless, both types of fire can last a long time. Jet flames are especially dangerous due to the high heat flux of this type of fire, leading to an equipment failure in a very short period of time (Casal, 2018).

1.2. Background: Major industrial accidents

Technological evolution experienced by the industrial sector, particularly the chemical industry, leads to the increasing inventory of chemical products in both facilities and transportation, nevertheless, this also increases the probability of major accidents occurring with a significant impact on society and the environment.

Vílchez et al. (1995) explain in an historical analysis that roughly 5,325 accidents occurred in chemical industry and in transportation of hazardous substances in the last decades of the 20th century. In this study, leaks of substances were among the most frequent type of accidents representing a 51%, fires are the second most frequent accidents occurring 44% of the time, followed by explosions at a 36% of occurrence, while the formation of a gas cloud only occurred 12% of the times. The accumulated frequency is greater than the 100% since this type of accidents can happen simultaneously in the same event.

For instance, in 1984, a series of explosions in a liquid petroleum gas (LPG) Storage Park at Mexico City consumed 11,000 cubic meters of LPG, representing one third of Mexico City's supply. Furthermore, these explosions destroyed the facility and devastated the local town of San Juan Ixhuatepec, leading to a total of 450 deceased people and roughly 6,000 others suffering severe burns (Arturson, 1987).

In the same year, a runaway reaction in a tank containing poisonous methyl isocyanate, in Bhopal, India, caused the pressure relief system to vent large amounts to the atmosphere giving rise to a toxic cloud that caused 3,000 causalities and 17,000 affected civilians (Eckerman, 2005).

Likewise, in Sao Paulo, Brazil, a gasoline leak at a favela left a body count of 800 people and a serious environmental problem in the nearby areas. Similarly, in 1989, an explosion and fire killed 23 and injured 314 people at Pasadena, Texas (Bethea, 1989).

Although several improvements in security protocols and safety amendments had been established since the last decades; major industrial disasters remain to be a problem in modern industries, especially in chemical and petrochemical sectors.

In 2012, at Mexico´s Gulf an explosion and subsequent fire resulted in the sinking of the Deepwater Horizon drilling rig, leading to a total of 11 causalities and 17 injuries. Nevertheless, the blowout that caused the explosion also caused a massive offshore oil spill in the Gulf of Mexico, considered to one of the largest accidental marine oil spills, and environmental disaster in the world (Goldenberg & MacAlister, 2012).

Furthermore, in Texas, USA an explosion occurred at the West Fertilizer Company storage and distribution facility in 2013, while emergency services personnel were responding to a fire at the facility. A total body count of 14 deceased, about 160 people were injured, and more than 150 buildings suffered either damage or were destroyed (Lateef, 2013).

Recently in 2015 a series of explosions at a container storage station, due to the auto-ignition of nitrocellulose, resulted in 173 deceased people, nearly 800 injured people and about 300 damaged buildings in the Port of Tianjin, China (Huang & Zhang, 2015)

These few examples prove that, even though the chemical industry has been established as an up growing sector in both technology and economic; the necessity of improving safety programs and security protocols its undeniable urgent to guarantee a sustainable development for society.

2. Objectives

The objective of this work is to statistically analyze the main geometrical features of transitory methane jet fires in subsonic regimes at different atmospheric conditions.
Furthermore, the specific objectives expected for this work are the following:

- Correlate experimental data of lift off distance, flame length, flame volume and flame diameter as function of different dimensionless variables.
- Determine the variation of geometrical features at different atmospheric pressure conditions.
- Compare experimental results against previous case studies regarding flame stability and mathematical models.

3. Theoretical Framework

3.1. Jet Flames: Geometrical Features

Jet flames are diffusion flames, meaning that the fuel and air are initially separate, while mixing occurs once the fuel is being release and ignition begins. High momentum above the outlet duct of the fuel, often a gas flowing at relatively high pressures, characterizes this type of fires (Palacios *et al.*, 2009).

The main geometrical features of jet flames are function of diverse variables such as the outlet nozzle diameter, jet fire exit velocity, mass flow rate, and release atmospheric pressure.

Lift off distance is the centerline distance from the gas release point to the start of detachment at a stabilized flame. Moreover, lift off distance is a function of diverse variables, such as jet flame exit velocity, outlet diameter and Froude number thus, various authors have tried to establish several mathematical expressions based on these variables (Palacios *et al.*, 2009).

Furthermore, lift off occurs by increasing the velocity for an ignited fuel jet attached to a nozzle above a certain critical velocity. Increasing the velocity causes the flame to move further downstream until it eventually blows off. Above a certain outlet orifice diameter blow off does not occur (Rokke et al., 1994).

At low speeds, where the flames are laminar, the height of the flame is independent of its initial diameter and depends solely on the volumetric flow, nevertheless, as flow increases, the turbulence begins to influence the height of the flame and a transition regime can be observed. In this transitional region, increasing levels of turbulence with the flow make the turbulent flames shorter than their laminar counterparts. As the flow increases, the flame lengths may remain essentially constant or increase at decreasing rates (Turns, 2000).

This occurs because the entrainment and air mixing speeds are proportional to the fuel flow, in addition, a significant dependence of the flame length on the initial diameter of the jet flame is observed.

The stability of the flame has many implications for practical applications. For example, the lift-off must be avoided so that the flame is close to the burner in order to ensure that the position of the flame is controlled.

3.2. Jet Flames: Previous case studies

Jet flames have been greatly studied for years due to its great importance in improvement of safety measurements and risk analysis in chemical industries. Although the direct effects of a fire dart are among the least severe of those found in fire accidents, they can often provoke a chain of events that ultimately amplifies the scale of destruction.

Wohl et al., (1949) study focuses mainly in the stability of open flames stability and the relation between this variable and flash-back, burning velocity, penetration distance, lift off distance and blow off.

Moreover, Kalghatgi (1984) studied the lift off distance and the visible flames for 4 different fuels at atmospheric pressure; suggesting that lift off distance varies linearly with the jet exit speed and establishing a relationship with Reynolds dimensionless number. Likewise, Rokke

et al., (1994) focused on the relationship of lift off distance, flame height and NO_x emissions between the outlet nozzle diameters of partially premixed propane flames.

McCaffrey & Evans (1986) analyzed large vertical methane flames (approximately 20 m in length) with nozzle diameters between 38 and 102 mm at atmospheric conditions. This work suggests that flame height is 200 times larger the nuzzle exit diameter at subsonic regime flames.

Nowadays, jet fires are still accidental fires of interest among risk assessment studies due to the high occurrence rate in either processing plants or in the transportation of hazardous materials. Nevertheless, these previous researches solely focus in jet flames main features at atmospheric conditions and at subsonic regimes; neglecting effect of pressure on jet flames geometrical traits.

Recent studies have related geometrical and thermodynamic traits of jet flames in more detail thus, have complimented last century studies.

Palacios et al. (2009) conducted experiments with propane flames up to 10 m in length, in sonic and subsonic flow rates at six different nozzle diameters. This research explains that flame height increases as both nozzle diameter and mass flow of fuel increase, as well as determining that the division of flame height between nozzle diameter equals 5.8 times the number of Reynolds raised to 0.27 power.

Wang et al. (2014) propane flame experiments vary atmospheric pressures from 60 kPa to 100 kPa at nozzle diameters from 4 to 6 mm. Results show that average flame height is higher at lower pressures. In addition, results also include that pressure decreases imply a lift-off distance increase, while the lifting speed decreases.

Furthermore, Hu et al. (2015) study confirms Wang et al. (2014) findings as these results also occurred at propane flame experiments varying atmospheric pressures at nozzle diameters from 4 to 10 mm.

Recently, the conjunction of stretched laminar flame modelling and experimental jet flame data, have led to more practical, generalized, correlations of experimental jet flame data, involving a dimensionless flow number, that is closely related to the Karlovitz stretch factor, employed in premixed turbulent combustion (Palacios et al., 2016).

As previously stated, many researches have proposed different accurate models and methodology to properly quantify geometrical and physical properties of jet flames. This work will solely focus in the effect of the flames that will be exposed under atmospheric and sub atmospheric pressures.

4. Methodology

The experiments are carried out in a designed laboratory facility to reveal the lift-off behavior of turbulent jet diffusion flames at sub-atmospheric pressures, ranging from 0.7 atmospheres to 1 atmosphere. The lift-off height data is then correlated and interpreted based on the dependency of turbulent flame speed at different pressures.

4.1. Experimental Setup

Figure 1 shows a schematic of the experimental facility and measurement equipment, located in Anhui, China.

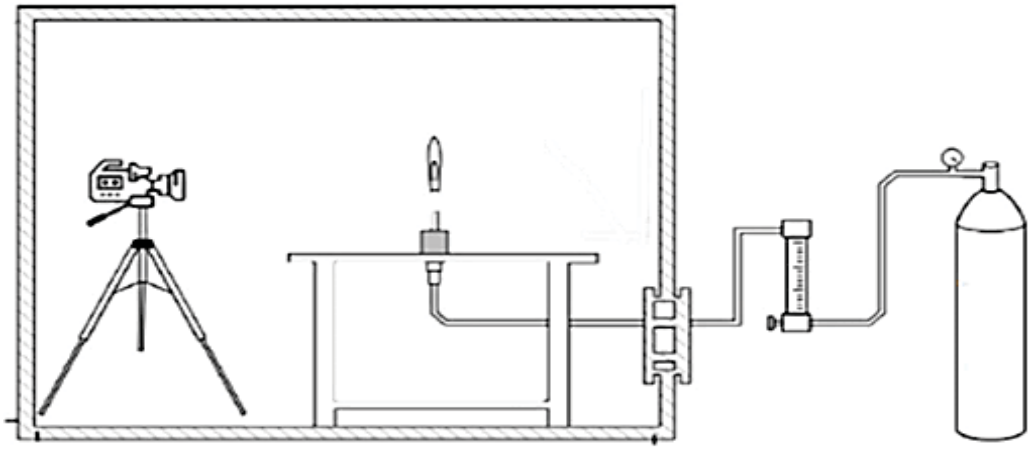

Figure 1 Experimental Facility in Anhui, China (Wang et al., 2014).

This setup is located at 50 meters above sea level, at an atmospheric pressure of 100 kPa; the instrumental equipment consists of a fuel supplying system connected through pipelines into a stainless-steel nozzle inside an air-pressurized chamber. The dimensions of this chamber are 3 meters in width, 2 meters in length and 2 meters in height at a constant temperature and ambient humidity of 24.9°C and 35% respectively. The pressure sensor within the chamber controls the air-pressurized into the installment by the vacuum pump; the pressures for the experiment are set at 0.7, 0.8, 0.9 and 1 atmospheres.

The methane flows at a rate of 10.24 liters per minute into the nozzle of 3 millimeters of diameter; each test starts to run once the pressure is constant in the chamber for a period of approximately 5 minutes. Moreover, the duration of each experimental condition is about 2 minutes, to ensure that the conditions within the chamber remain constant. Subsequently, once the test run is completed the experimental condition of the following pressure starts by pumping fresh air into the chamber to replace the air from the previous test.

4.2. Experimental Measurement & Regression Analysis

A digital charge-coupled device (CCD) camera with a sensor size of 8.5 millimeters and resolution of 3.0 megapixels visualizes and films the flame, at a speed of 25 frames per second. An average method allows to objectively quantify the lift-off height based on the recorded image series, as there are still some fluctuations of the lifted flame base. Furthermore, time series flame video records are decompressed into frames and processed into single images for each test.

A total of 750 images from each test are converted to gray scale images for statistical analysis. This statically analysis determines the flame intermittency distribution by averaging the values of these images in each pixel position.

Figure 2 shows an example of the intermittency distribution of the flame. By doing this method, different structures of the flame can be identified such as the total height (H), the radiant height (h), the average flame diameter (D_{ave}), and lift-off (L). The sum of radiant length (h) and lift off distance (L) results in the total flame length (H). The lift-off height results are obtained by calculating the distance between the nozzle and the base of the flame; this method provides more objective quantification of the lift-off heights than visual observations.

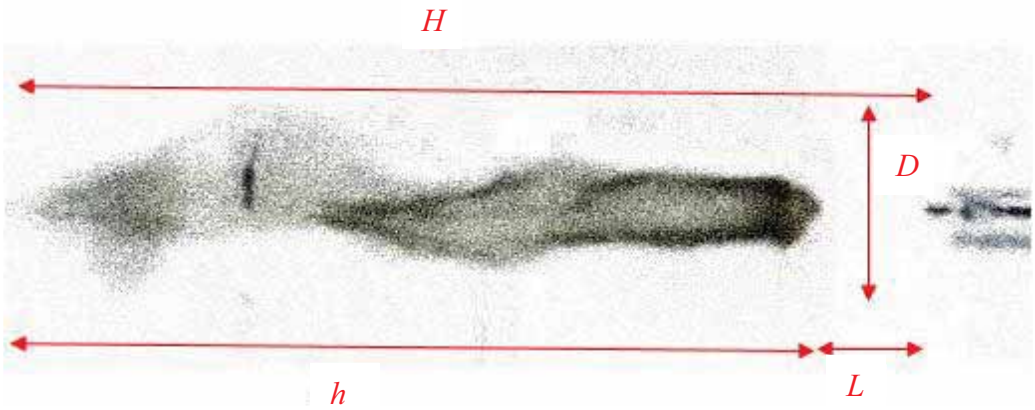

Figure 2 Main Geometrical Features identification at an infrared Jet Flame

To obtain the average diameter of each flame, the flame diameters are measure from the base to the maximum flame height. Figure 3 illustrates an example of the diameter measurement of a flame at sub-atmospheric pressure.

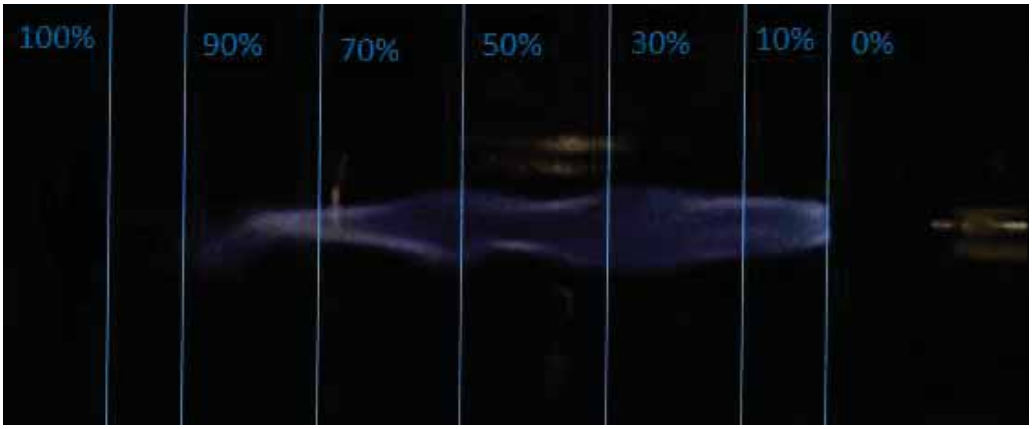

Figure 3 Methodology to measure flame diameter at different Jet Flame sections

For this study, the measurements of diameter in the flames are calculated from the base to the maximum height of each flame at different sections; 10%, 30%, 50%, 70%, and 90% of the total height to calculate the arithmetic average of the flare by parts.

These geometric parameters are compared between different dimensionless numbers to characterize the behavior of jet flames at different pressures.

The volume of the flame (V) is calculated from the integration of a polynomial regression of the curve of the flame square diameter (D^2) and flame heights from base to end.

Equation (1) describes the model used, where x_i are empirical constants attained from each regression model.

$$V = \int_{h_{0\%}}^{h_{100\%}} [x_3 h^4 + x_2 h^3 + x_1 h^2 + x_0 h]\ dh \quad (1)$$

Equation (2) calculates the Reynolds number to characterize the movement and type of fluid model where D is the nozzle diameter, v kinematic viscosity and u fuel velocity.

$$Re = \frac{uD}{v} \quad (2)$$

With further increases in jet velocity, more air is entrained, localised equivalence ratios fall as the mixture leans off, and flame extinction stretch rates decrease, to the extent that eventually all flamelets are extinguished and the flame blows off. Computations of the distributions of equivalence ratios show that at flow veloci-ties, before approaching blow-off, the peak value in probability density function is close to that for the maximum burning velocity of the mixture. This supports the widespread use of the maximum value of the laminar burning velocity of the mixture, S_L, in dimensionless groups for correlating lift-off distance and main geometrical features. The stretched laminar flamelet modelling in conjunction with experimental jet flame data, have led to more practical, generalized, correlations of experimental jet flame data, involving a dimensionless flow number, U^*, that is closely related to the Karlovitz stretch factor, employed in premixed turbulent combustion.

Equation (3) determines the pressure dependence of the burning velocity of the fuel at laminar regime from atmospheric conditions of 0.5 atm to 20 atm as given by Agnew & Graiff (1961).

$$S_L = 32.9 - 6.78 \cdot ln(P_o) \quad (3)$$

Where P_o it's the atmospheric outlet pressure in Pascal.

Likewise, Palacios et al. (2016) suggests Equation (4) as a dimensionless flow number considering combustion and burning factors related to the Karlovits stretch factor.

$$U^* = \left(\frac{u}{S_L}\right) \cdot \left(\frac{P_i}{P_o}\right) \cdot \left(\frac{D}{v\ S_L^{-1}}\right)^{-0.4} \quad (4)$$

5. Results & Discussions

From the analysis of both the visible and infrared images and the suggestion of different authors; the geometry of the vertical jet fires in still air will be approximated to that of a cylinder (Santos & Costa, 2005).

A dimensional analysis is carried out to correlate the experimental results. The experimental variables: lift off distance (L), visible flame length (h), total flame length (H), average flame diameter (D_{ave}) and average flame volume (V) are to be correlated as functions of atmospheric outlet pressure (P_o), the Reynolds number (Re), and the dimensionless flow number for choked and unchoked flow(U^*).

Finally, by doing the correlation between these variables, a set of mathematical expressions that predict jet flames geometrical traits are suggested.

5.1. General Parameters & Results

General experimental parameters that remain constant or vary as a function of pressure are presented in Table 1

Table 1 General experimental parameters.

Parameter	Pressurized Conditions			
P_o (atm)	0.7	0.8	0.9	1
V_f (m^3/s)	$1.707 \cdot 10^{-04}$			
D (m)	0.003			
A (m^2)	$7.069 \cdot 10^{-06}$			
u (m/s)	24.14			
Fr	19814.85			
υ_{Mixed} (m^2/s)	$2.27 \cdot 10^{-05}$	$1.98 \cdot 10^{-05}$	$1.76 \cdot 10^{-05}$	$1.59 \cdot 10^{-05}$
υ_{CH4} (m^2/s)	$2.76 \cdot 10^{-05}$	$2.42 \cdot 10^{-05}$	$2.15 \cdot 10^{-05}$	$1.93 \cdot 10^{-05}$
S_L (cm/s)	35.32	34.41	33.61	32.90
Re	2621.85	2997.14	3372.99	3748.27
U^*	11.72	11.27	10.91	10.61

In this case study, flow rate (V_f) and nozzle diameter (D) remain constant thus, outlet fuel velocity (u), transversal pipeline area (A) and Froude number (Fr) remain unchanged. However, as pressurized conditions changed throughout experimental runs dynamic viscosity (υ) varies; resulting on Reynolds number (Re), burning fuel velocity (S_L) and the dimensionless flow number(U^*) to be dependent of pressure conditions.

Table 2, presents the overall results from the experimental measurements of jet flames geometrical traits from 0.7 atm to 1 atm. The geometrical features of interest for this study are lift off distance, radiant flame height, flame diameter and flame volume. For each parameter, the average of 749 data measured its presented.

Table 2 Main geometrical jet flames features

Parameter	Pressurized Conditions			
P_o (atm)	0.7	0.8	0.9	1
L (cm)	8.376	6.745	4.728	0.000
H (cm)	49.527	52.131	53.487	50.412
h (cm)	41.151	45.386	48.759	50.412
V (cm^3)	1460.824	1396.085	1335.080	1398.231
D_{ave} (cm)	5.153	4.742	4.280	4.079
σ_L (cm)	1.036	0.544	0.371	0.000
σ_H (cm)	4.887	4.892	4.168	4.814
σ_h (cm)	5.163	5.014	4.153	4.814
σ_V (cm^3)	291.571	289.263	399.975	343.718
σ_{Dave} (cm)	0.547	0.513	0.556	0.448

These parameters will be normalized to D to obtain dimensionless sets of equations as a function of different variables. The correlation of these parameters are presented for each geometrical trait.

5.2. *Lift off distance*

A common trend was observed for the subsonic flow range when normalized lift off distance (L/D) were plotted as a function of P_o, Re and U^*.

The variation in lift off distance as a function of pressure is analyzed in Figure 4.

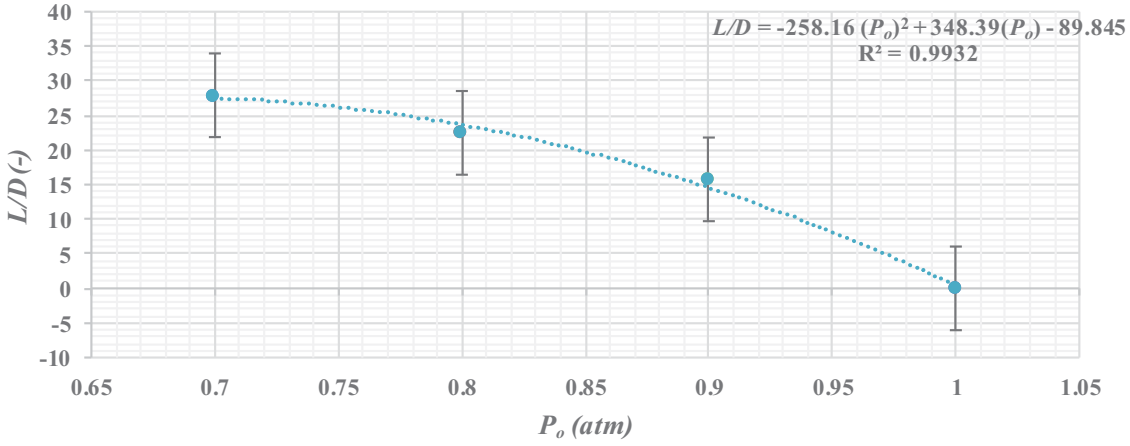

Figure 4 Correlation in L/D as function of P_o.

In this case lift off distance is nonexistent at 1 atm, moreover, the correlated experimental data indicates that lift off distance increases when atmospheric pressure decreases.

Equation (5) is obtained from a quadratic regression model of the experimental data.

$$\frac{L}{D} = -258.16 \cdot (P_o)^2 + 348.39 \cdot (P_o) - 89.845 \quad (5)$$

In Figure 5, the variation of *L/D* as a function of *Re* is statistically analyzed.

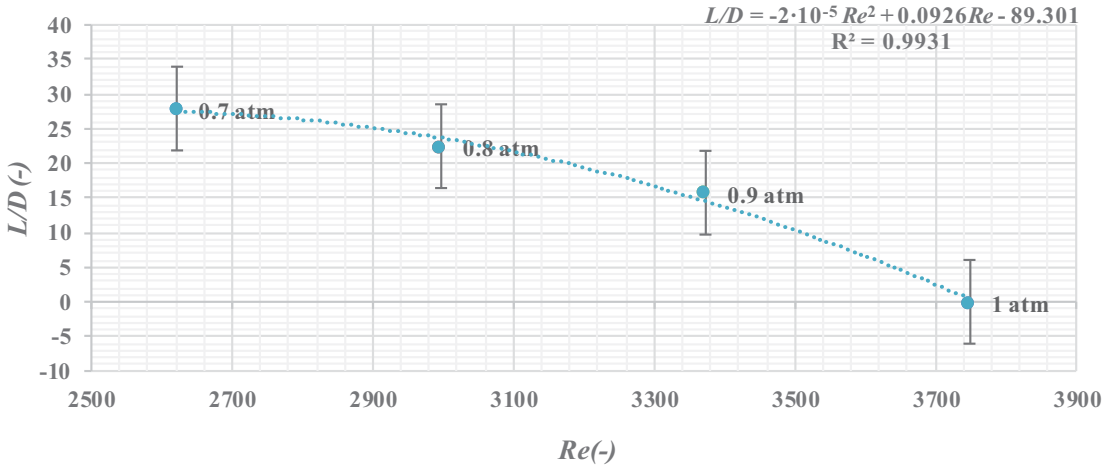

Figure 5 Correlation of L/D as function of Re.

The relationship between *L/D* as function of *Re* is expected to be like Figure 4 because *Re* depends on thermodynamic parameters. In this case, as *Re* increases *L* decreases; meaning that as the jet flame gains more turbulence the lift off distance decreases being nonexistent at 1 atm.

An expression for predicting *L* as a function of *Re* its obtained in Equation (6):

$$\frac{L}{D} = -(2\cdot10^{-5})\cdot Re^2 + 0.0926\cdot Re - 89.301 \quad (6)$$

In a similar manner, values of *L/D* are plotted against U^* in Figure 6 to analyze the correlation and relationship between these variables.

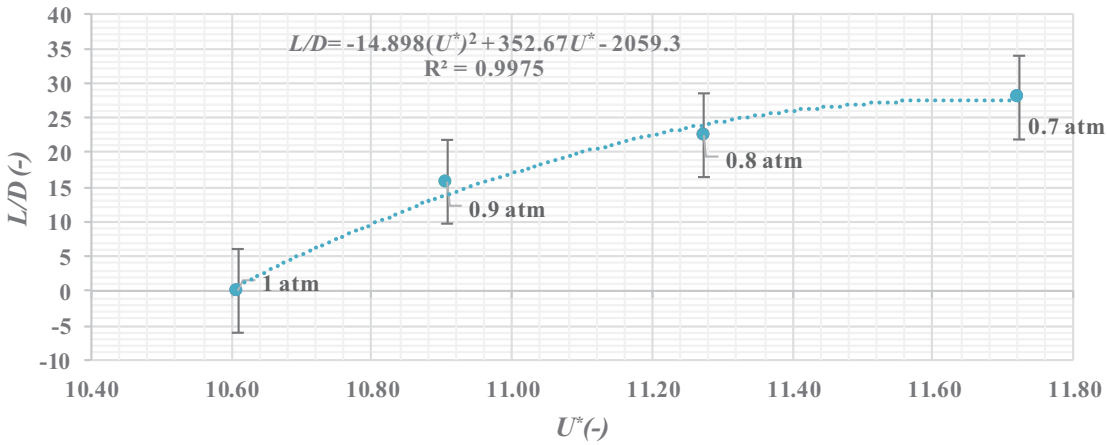

Figure 6 Correlation of L/D as function of U^*.

A quadratic regression model describes the variation of *L/D* as function of U^*. In this correlation, as U^* increases *L* also increases. This relationship indicates that as U^* increases due to the burning velocity of the fuel (S_L) decreases, since U^* is inversely proportional to S_L and depends on thermodynamic properties

Equation (7) is obtained by the quadratic regression model that describes *L/D* as a function of U^*.

$$\frac{L}{D} = -14.898 \cdot (U^*)^2 + 352.67U^* - 2059.3 \quad (7)$$

Comparing the analysis of each variation of this parameter; it can be established that lift off distance is a geometrical trait of jet flames that is in fact affected by different pressure conditions. The mathematical models previously presented in this section adjust properly to the experimental data; in which these models have a correlation coefficient (R^2) approximately equal to 1. This is similar to Wang et al. (2014) propane flame experiments that determined that pressure decrease imply a lift-off distance increase, while the lifting speed decreases.

5.3. Visible Flame Height

An analysis between normalized visible flame height (*h/D*) as a function of P_o, *Re* and U^* is included in this section.

In Figure 7, *h/D* is plotted as a function of P_o to analyze the relationship between both variables.

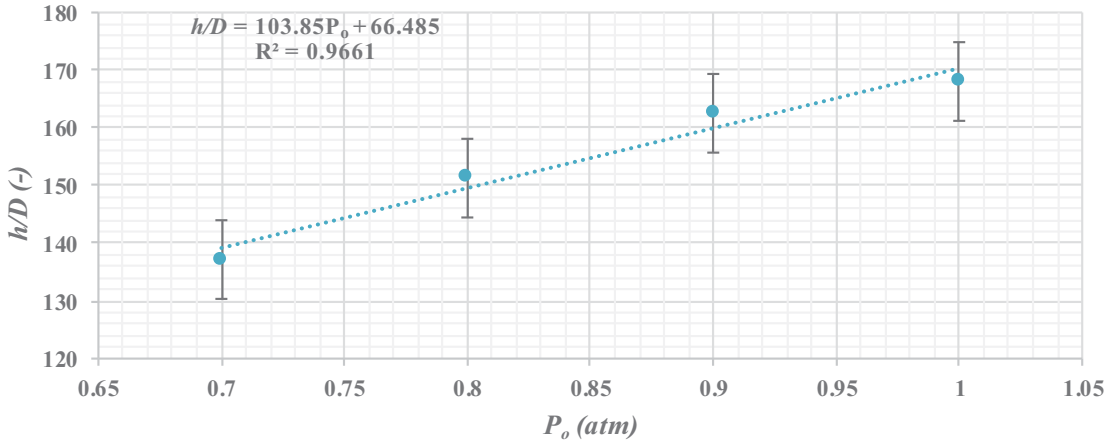

Figure 7 Correlation in h/D as function of P_o.

This correlation indicates that *h/D* adjust to a lineal model that is proportional to P_o, meaning that as the atmospheric pressure increases the visible flame height also increases.

Equation 8 describes this regression model.

$$\frac{h}{D} = 103.85 \cdot P_o + 66.485 \quad (8)$$

The variation of *h/D* as a function of *Re* is described in Figure 8.

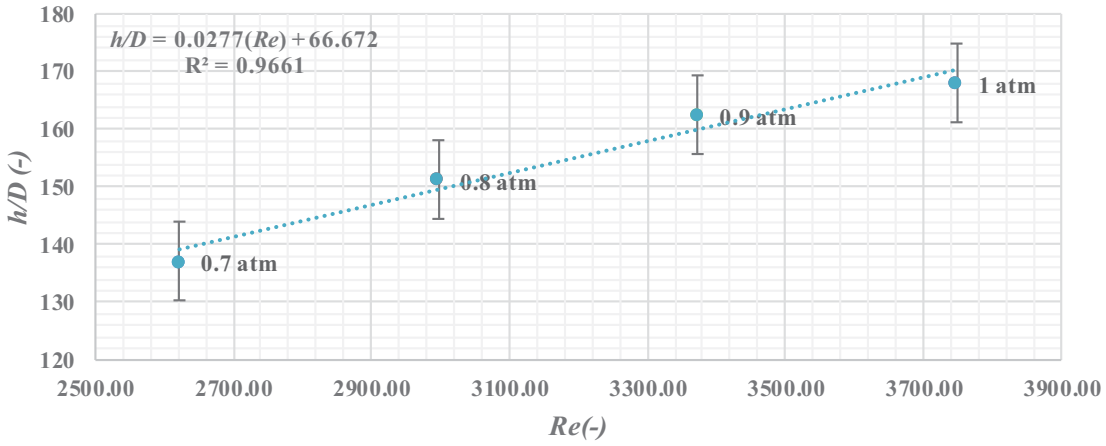

Figure 8 Correlation of h/D as function of Re.

In a similar manner to *L/D*, the relationship between *h/D* as function of *Re* is also expected to be like that of Figure 7 due to *Re* dependency on thermodynamic parameters. In this case, as *Re* increases *h* increases as well; meaning that as the flame gets more turbulent the visible area of the jet flames increases.

The previous relationship is described in Equation 9.

$$\frac{h}{D} = 0.0277 \cdot Re + 66.672 \quad (9)$$

Moreover, the correlation of the experimental data of *h/D* as a variable of U^* is presented in Figure 9.

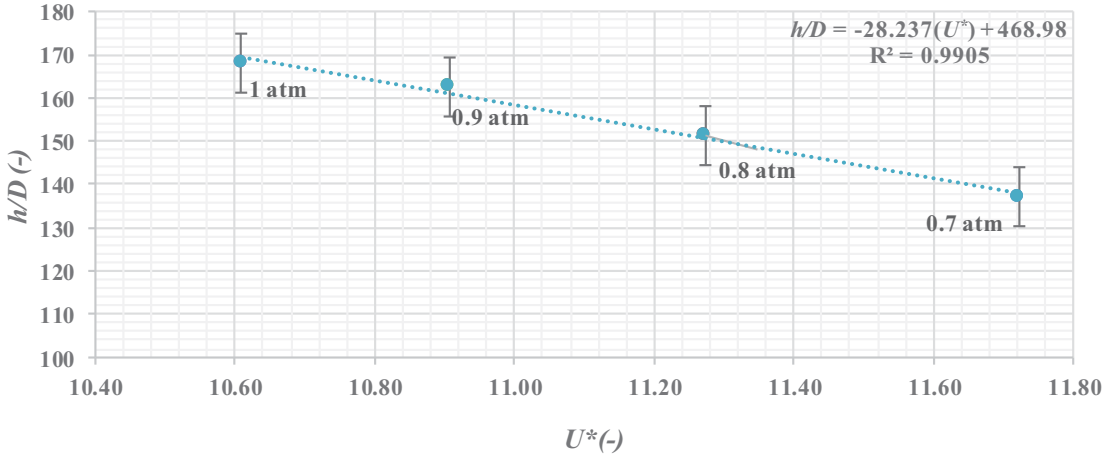

Figure 9 Correlation of h/D as function of U^*.

This correlation also fits a lineal regression model in which, as U^* increases *h* decreases. This variation indicates that as U^* increases because S_L decreases, since U^* is inversely proportional to S_L and depends on atmospheric conditions.

Equation (10) describes *h/D* as a function of U^* as a simplified quadratic model.

$$\frac{h}{D} = -28.237U^* + 468.98 \quad (10)$$

The visible flame height is also a geometrical trait of jet flames that that can be described as a function of atmospheric pressure conditions. In this case the visible flame height is directly proportional to outlet pressure as the empirical expressions presented in this section also adjust properly to the experimental data due to R^2 being nearly equal to 1. Likewise, Wang et al. (2014) propane flame results show that average flame height is higher at lower pressures.

5.4. Total Flame Height

The sum of the visible height length (*h*) and lift off distance (*L*) results in the total flame length (*H*). In this case study, to determine the total flame length the measurement from the base of the lifted flame to the flame tip was performed. In this case the reported experimental total flame corresponded to the timed-averaged values.

The normalized total flame height (*H/D*) is correlated as a function of P_o as shown in Figure 10.

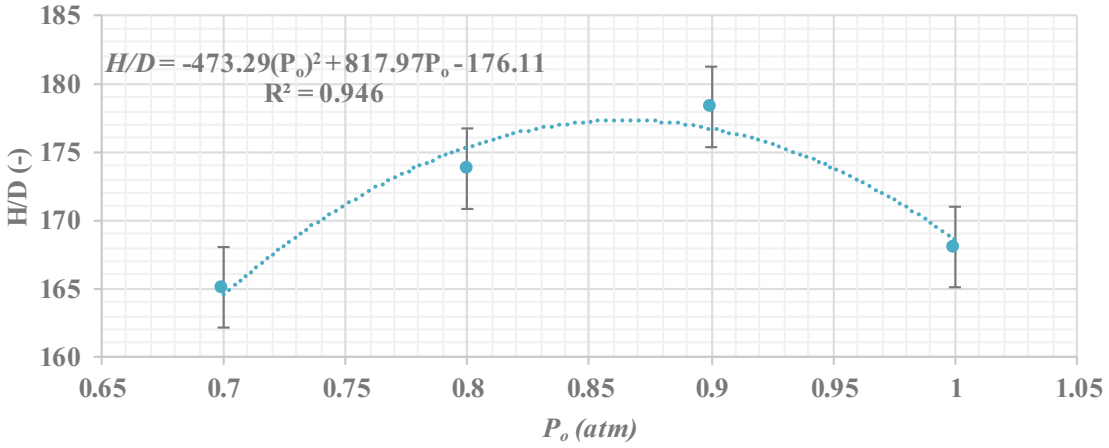

Figure 10 Correlation in H/D as function of P_o.

This correlation shows that *H/D* can be adjusted to a quadratic regression model as a function of P_o. In this case, the maximum total flame height is achieved at 0.9 atm because at 1 atm there is not lift off distance; meaning that as pressure increases from 0.9 atm the visible flame length (*h*) approximates more to the total flame height (*H*).

Thus, the normalized total flame height at different atmospheric pressure can be model from the following Equation 11.

$$\frac{H}{D} = -473.29\cdot(P_o)^2 + 817.97\cdot(P_o) - 176.11 \quad (11)$$

In Figure 11 the correlation of *H/D* as a function of *Re* is presented.

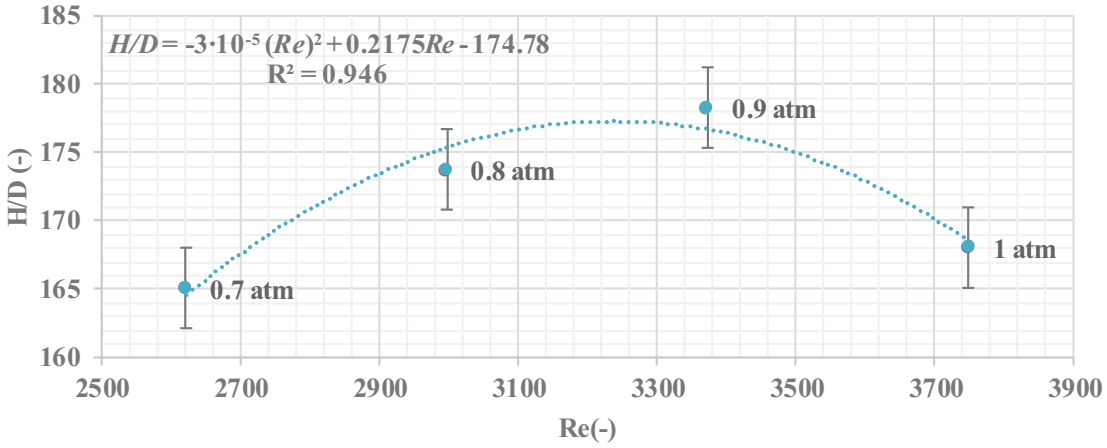

Figure 11 Correlation in H/D as function of Re.

As of previous *Re* correlation analysis, the relationship between *H/D* as function of *Re* is also like that of Figure 10 due to *Re* dependency on thermodynamic properties. In this case study, as *Re* increases *H/D* also increases reaching the maximum value of *H/D* when *Re* is nearly 3500 at 9 atm, then *H* its approximately equal to *h*; meaning that as the flame gets more turbulent and more pressurized the visible flame height is also the total flame height.

Equation 12 describes the relationship of *H/D* as a function of *Re*.

$$\frac{H}{D} = -(3\cdot10^{-5})\cdot Re^2 + 0.2175\cdot Re - 174.78 \quad (12)$$

In Figure 12 the variation of *H/D* as a function of U^* is described.

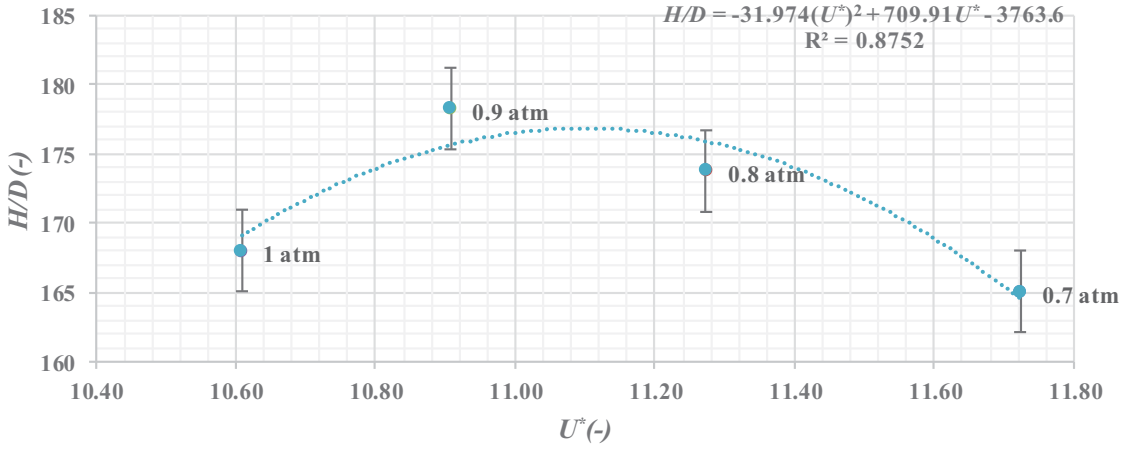

Figure 12 Correlation in H/D as function of U^*.

This correlation adjusts to a quadratic regression model, from which from 0.9 atm to 1 atm as U^* increases *H* also increases reaching the maximum value at 0.9 atm then as U^* increases the total flame height starts to decrease. This relationship indicates that when S_L increases the

total flame height decreases since S_L depends on thermodynamic properties; as atmospheric pressure increases S_L decreases.

Moreover, Equation (13) describes *H/D* as a function of U^*.

$$\frac{H}{D} = -31.974\cdot(U^*)^2+709.91U^*-3763.6 \quad (13)$$

By the analysis of each correlation for this parameter; it can be established that total flame height is also a geometrical trait of jet flames that is affected by different pressure conditions. The mathematical models previously presented in this section adjust properly to the experimental data because whereas R^2 roughly equal to1.

5.5. Flame Diameter

The correlation for the normalized average flame diameter (D_{ave}/D as a function of P_o is shown in Figure 13.

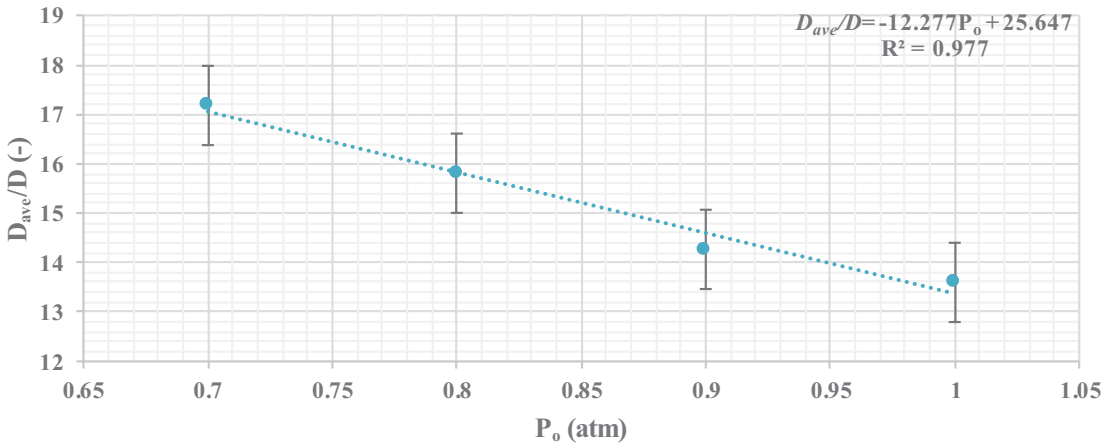

Figure 13 Correlation in D_{ave}/D as function of Po

In this case, a lineal regression model adjusts best the correlated experimental data. At an atmospheric pressure of 1 atm the average flame diameter presents the minimum value, moreover, this model indicates that when atmospheric pressures increase the flame diameter decreases.

The previous relationship is described in Equation 14.

$$\frac{D_{ave}}{D} = -12.277\cdot(P_o)+25.647 \quad (14)$$

The correlation of D_{ave}/D as a function of *Re* is described in Figure 14

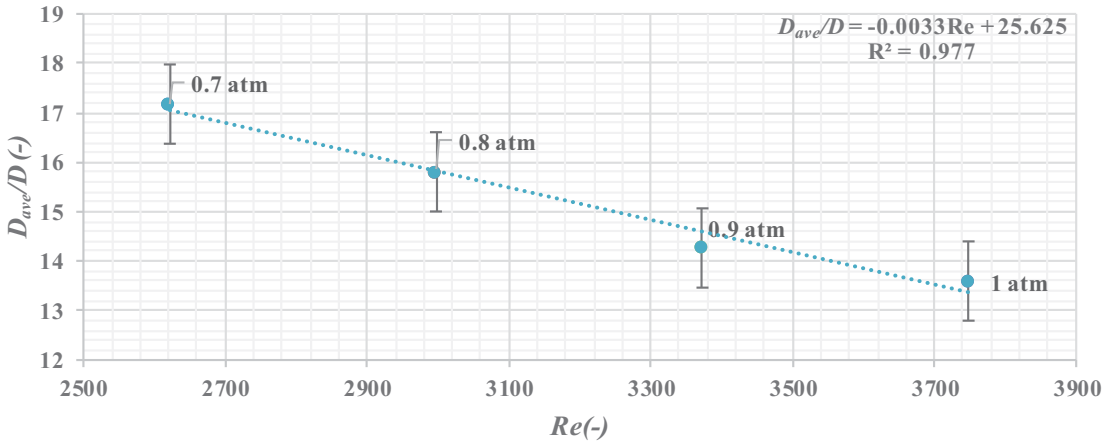

Figure 14 Correlation in D_{ave}/D as function of Re

Similarly, this case *Re* correlation analysis indicates a relationship between D_{ave}/D as function of *Re* like that of Figure 13 because of *Re* variability due to thermodynamic properties. In variation as *Re* increases D_{ave}/D also decreases; meaning that as fluid turbulence and at pressurized conditions the flame overall diameter decreases.

Equation 15 suggests a quadratic model for D_{ave}/D as a function of *Re*.

$$\frac{D_{ave}}{D} = -0.0033 \cdot Re + 25.625 \quad (15)$$

Furthermore, the correlation of the experimental data of D_{ave}/D as a variable of U^* is presented in Figure 15.

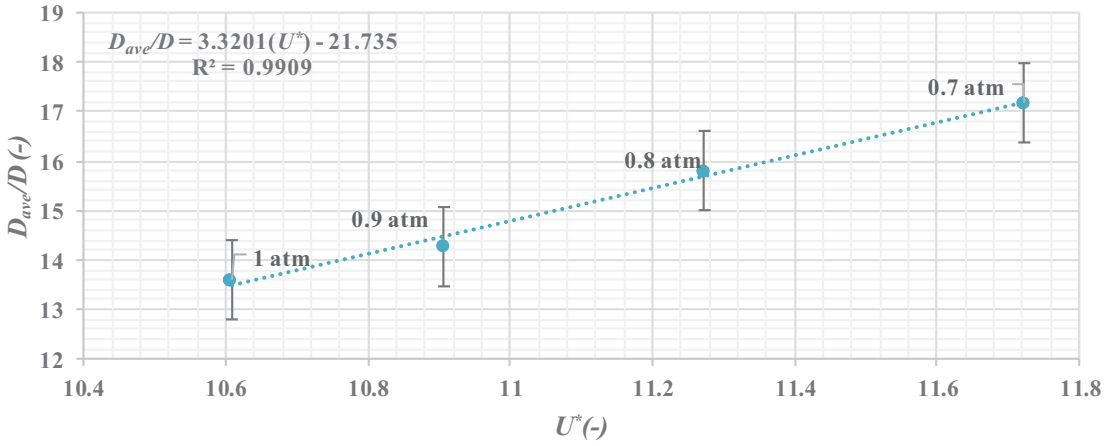

*Figure 15 Correlation in D_{ave}/D as function of U**

The correlation indicates that a lineal regression model describes the variation of D_{ave}/D as function of U^*. In this correlation, as U^* increases D_{ave} also increases. This relationship indicates that as S_L decrease overall flame diameter increases since U^* is inversely proportional to S_L; parameter that depends on thermodynamic properties.

Equation (16) is obtained by the lineal regression model that describes D_{ave}/D as a function of U^*.

$$\frac{D_{ave}}{D} = 3.3201 \cdot U^* - 21.735 \quad (16)$$

From this analysis, it can be established that average flame diameter is a geometrical trait that is dependent of pressure conditions. The lineal models suggested in this section adjust properly to the experimental data as R^2 is approximately equal to 1. Moreover, Wang et al. (2014) propane flame.

5.6. *Flame Volume*

A common trend is observed when normalized average flame volume (V/D^3) is plotted as a function of P_o, Re and U^*. Equation 1 is applied to calculate V approximating it to a cylindrical geometry.

Therefore, Figure 16 shows the variation of V/D^3 as a function of P_o.

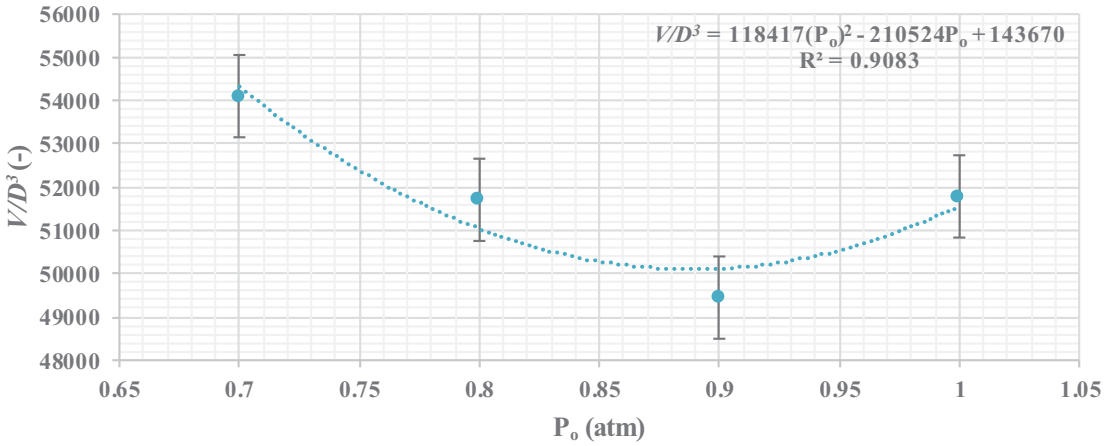

Figure 16 Correlation of V/D^3 as function of P_o.

This correlation fits a quadratic regression model as a function of P_o. In this case, the maximum flame volume is at 0.7 atm and the minimum at 0.9 atm; meaning that as pressure increases from 0.7 atm to 0.9 atm V decreases, meanwhile, as pressure increases from 0.9 atm to 1 atm the overall flame volume increases.

From a quadratic regression model of the experimental data Equation (17) is obtained.

$$\frac{V}{D^3} = 118{,}417 \cdot (P_o)^2 - 210524 \cdot (P_o) + 143670 \quad (17)$$

In Figure 17, the variation of V/D^3 as a function of Re is statistically analyzed.

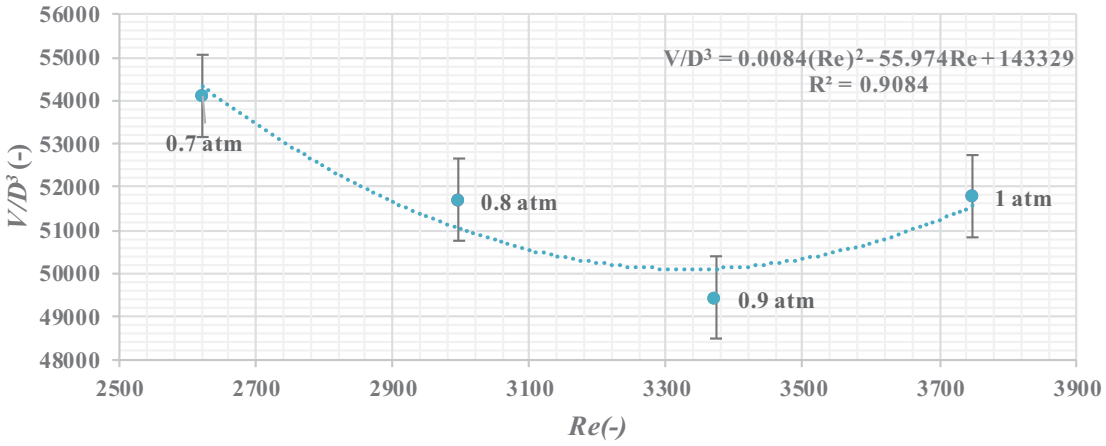

Figure 17 Correlation of V/D^3 as function of Re

As of previous Re correlation analysis, the relationship between V/D^3 as function of Re is also like that of Figure 16 due to Re dependency on pressurized conditions. In this case, when Re increases V/D^3 decreases from 0.7 atm to 0.9 atm reaching the maximum value when Re is nearly 3400 at 0.9 atm, then from 0.9 atm to 1 atm as turbulence increases flame volume also increases.

Equation 18 describes the relationship of V/D^3 as a function of Re.

$$\frac{V}{D^3} = (0.0084)\cdot Re^2 - 55.974\cdot Re + 143329 \quad (18)$$

In Figure 18 correlation of the experimental data of V/D^3 as a variable of U^* is presented.

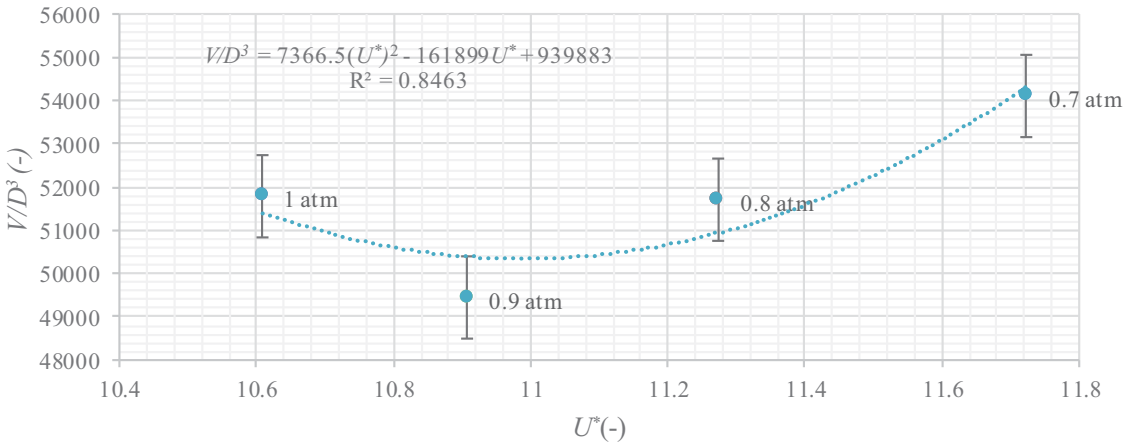

Figure 18 Correlation V/D^3 as function of U^*

This correlation adjusts to a quadratic regression model, from which from 1 atm to 0.9 atm as U^* increases V decreases reaching the minimum value at 0.9 atm, then as U^* increases V increases. This relationship indicates that U^* increases because S_L decreases since S_L depends on thermodynamic properties such as pressure.

Likewise, Equation (19) describes V/D^3 as a function of U^*.

$$\frac{V}{D^3} = (7366.5)\cdot(U^*)^2\text{-}161899\cdot U^* + 939883 \quad (19)$$

It can be established that flame volume is a geometrical trait of jet flames that is affected by different pressure conditions. The mathematical models previously presented in this section adjust to the experimental data, nevertheless, in this case an improvement in methodology is suggested to minimize measurement errors because R^2 for all analysis are approximately 0.9.

6. Conclusions

This paper reports an experimental investigation of geometrical features of methane jet diffusion flames in sub-atmospheric pressures. The dependency of these features is interpreted based on a laminar flame speed.

Major findings regarding methane jet flames geometrical traits are:

- Lift-off distance is higher in the sub-atmospheric pressures than that in normal pressure. Moreover, a lift off distance quadratic regression model dependent on pressure is proposed that could be applied at a range of 0.7 atm to 1 atm.
- The visible flame height has a lineal dependency on pressure, meaning that as pressure increases visible flame height also increases. A lineal regression model is proposed by including such pressure dependency function.
- Total flame height experimental data show that as pressure increases from 0.7 atm to 0.9 atm, the maximum value is reached at 0.9 atm. Moreover, when pressure increases more than 0.9atm the total flame height starts to be equal to the visible flame height because lift off distance decreases.
- The average flame diameter fits an inverse lineal regression model dependent on pressure, meaning that as pressure increases flame diameter decreases. A lineal regression model is proposed by including this relationship.
- Flame volume is also a geometrical trait affected by pressure conditions, nevertheless, the mathematical model suggested in this paper should be improved to minimize error as R^2 had a significant deviation from 1.

Further research of this case study is strongly suggested such as running experiments at both different or the same atmospheric conditions, varying type of fuel and air mixture. In conclusion, the objectives of this research where accomplished and future works should complement this investigation.

Acknowledgments

This work was supported by Universidad de las Americas Puebla (UDLAP) and Faculty Member A. Palacios-Rosas PhD research team. Author J. Garcia-Hilarios acknowledges financial support for his BSc studies in Chemical Engineering and Environmental Engineering from UDLAP.

Nomenclature

D_{ave}	Average Flame Diameter, cm
D_{ave}/D	Normalized Average Flame Diameter
D_{mac}	Maximum Flame Diameter, cm
D_{max}/D	Normalized Maximum Flame Diameter
D	Nozzle Diameter, mm
Fr	Froude Number
g	Gravity acceleration m/s^2
H	Total Flame Height, cm
h	Visible Flame Height, cm
H/D	Normalized Total Flame Height
h/D	Normalized Visible Flame Height
L	Lift off Distance, cm
L/D	Normalized Lift off distance
Pi	Initial stagnation pressure, Pa
Po	Atmospheric pressure, Pa
R^2	Correlation coefficient
Re	Turbulent Reynolds Number
S_L	Maximum laminar burning velocity of the fuel air mixture under atmospheric conditions, m/s
u	Fuel exit velocity, m/s
U^*	Dimensionless flow number for choked and unchoked flow
V	Average Flame Volume, m^3
V/D^3	Normalized Average Flame Volume
V_f	Volumetric flow (m^3/s)
x_i	Polynomial regression constants

Greek symbols

υ	Kinematic viscosity, m^2/s
σ	Standard Deviation

References

Arturson G. (1987). The tragedy of San Juanico-the most severe LPG disaster in history. *Burns, Including Thermal Injury*. 13 (2). 87-102.

Agnew J., & Graiff L. (1961) The pressure dependence of laminar burning velocity by the spherical bomb method. *Combustion and Flame*. 5, 209-219.

Bethea R. (1989). *Explosion and Fire at the Phillips Company Houston Chemical Complex*. Pasadena,TX. Chemical Engineering Department. Texas Tech University.

Casal J. (2018*). Evaluation of the Effects and Consequences of Major Accidents in Industrial Plants*. 2nd ed. Elsevier, 405-437.

Darbra R.M., Palacios A. & Casal J. (2010).Domino effect in chemical accidents: Main features and accident sequences. *Journal of Hazardous Materials*. 183(3). 565-573,

Eckerman, I. (2005). *The Bhopal Saga—Causes and Consequences of the World's Largest Industrial Disaster*. India: Universities Press.

Goldenberg, S. & MacAlister, T. (2012). "BP suspended from new US federal contracts over Deepwater disaster". *The Guardian*. London.

Hu, L., Zhang, X., Wang, Q., y Palacios, A. (2015). Flame size and volumetric heat release rate of turbulent buoyant jet diffusion flames in normal- and sub-atmospheric pressure. *Fuel, 150*, 278-287.

Huang, P. & Zhang, J. (2015). "Facts related to August 12, 2015 explosion accident in Tianjin, China". *Process Safety Progress*. 34 (4): 313–314.

Kalghatgi, G.T. (1984). Lift-Off Heights and Visible Lengths of Vertical Turbulent Jet Diffusion Flames in Still Air. *Combustion Science and Technology, 41*, 17-29.

Lateef M. (2013). "Explosion hits fertilizer plant north of Waco, Texas". *CNN*. United States of America.

Palacios, A., Muñoz, M., & Casal, J. (2009). Jet Fires: An experimental Study of the Main Geometrical Features of the Flame in Subsonic and Sonic Regimes. *AIChE Journal, 55 (1)*, 256-263.

Palacios, A., Bradley, D. & Hu L. (2016). Lift-off and blow-off of methane and propane subsonic vertical jet flames, with and without diluent air. *Fuel*. Volume 183.414-419.

Rokke, N.A., Hustad, J.E., y Sonju, O.K. (1994). A Study of Partially Premixed Unconfined Propane Flames. *Combustion and Flame, 97(1)*, 88-106.

Santos A. & Costa M. (2005). Reexamination of the scaling laws for NOx emissions from hydrocarbon turbulent jet diffusion flames. *Combustion and Flame. 142(1). 160-169.*

Turns, S.R. (2000). *An Introduction to combustion: concepts and applications*. Pennsylvania, Mc Graw-Hill, 2 Ed.

Vilchez, J.A., Sevilla, S., Montiel, H., & Casal, J. (1995). Historical analysis of accidents in chemical plants and in the transportation of hazardous materials. *J. Loss Prev. Process Ind., 8(2)*, 87-96.

Wang, Q., Hu, L., Zhang, M., Tang, F., Zhang, X., y Lu, S. (2014). Lift-off jet diffusion flame in sub-atmospheric pressures: An experimental investigation and interpretation based on laminar flame speed. *Combustion and Flame, 161*, 1125-1130.

Wohl, K., Gazley, C., & Kapp, N. (1949). Diffusion Flames. *Proc. Combustion Flame and Explosions Phenomena, 3*, 388-300.